

Kinetic simulations of electron-scale magnetic  
reconnection in space plasma turbulence (pr27ta)  
SuperMUC Status and Results Workshop 2023  
LRZ Garching/online

**Patricio Muñoz**  
Jörg Büchner

Max Planck Institute for Solar System Research, Göttingen, Germany  
Center for Astronomy and Astrophysics, Technical University Berlin, Germany



10th May 2023

# Contents

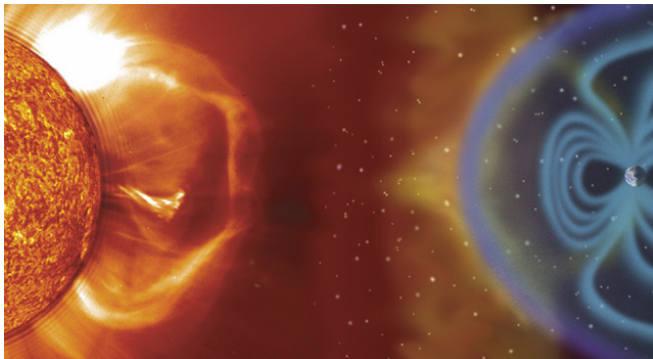
- 1 Introduction
- 2 Method
- 3 Results
- 4 Conclusions

# Contents

- 1 Introduction
  - Introduction
- 2 Method
- 3 Results
- 4 Conclusions

# Space plasmas

- Most of our space environment, solar corona, solar wind, planetary magnetospheres is a **collisionless** plasma.
- Collisionless plasmas have particles with large mean free path  $\Rightarrow$  Large deviations from **thermal equilibrium**  $\Rightarrow$  Kinetic (not fluid) approach is necessary.





# Turbulence in space plasmas

- Space plasmas are often turbulent, with features deviating from fluid (MHD: Magnetohydrodynamic models) at particle scales.

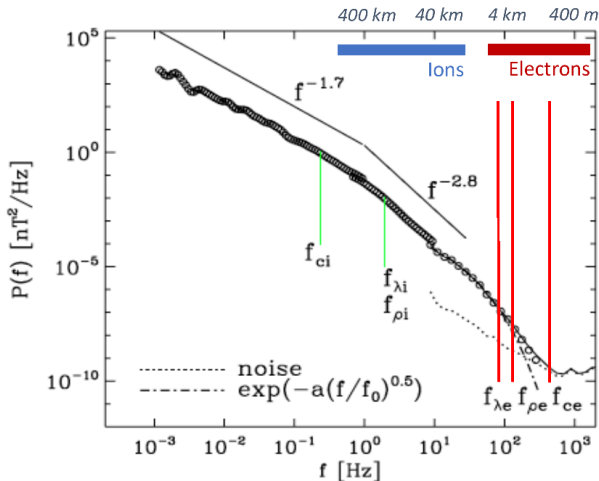


Figure 1: Turbulent magnetic spectra in the solar wind measured with the Cluster spacecraft [Verscharen 2019]  
Patricio Muñoz (munozp@mps.mpg.de)

# Magnetic Reconnection

## Magnetic Reconnection

- **Fast** ( $\ll$  diffusive  $\tau$ ) magnetic energy release.
- Change of magnetic field **topology**.
- Conversion of magnetic energy to **particle energy** (flows, heating, acceleration)
- Responsible for solar flares, magnetic storms in planetary magnetospheres, but also present in plasma turbulence.

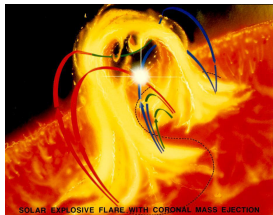


Figure 2: Schematics of a solar flare

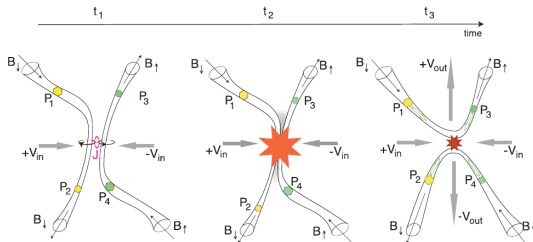


Figure 3: Schematics of Reconnection [Treumann and Baumjohann, 2013]

# Turbulence and Magnetic Reconnection

## Turbulence and Magnetic Reconnection

- Turbulence  $\Rightarrow$  magnetic reconnection through current sheets.
- This phenomena has been observed in MHD simulations since the 80s.

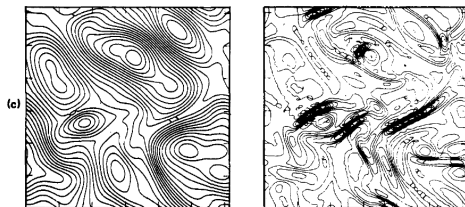


Figure 4: Decaying MHD turbulence. Left: Magnetic field lines. Right: Current density. [Matthaeus and Lamkin, 1986]

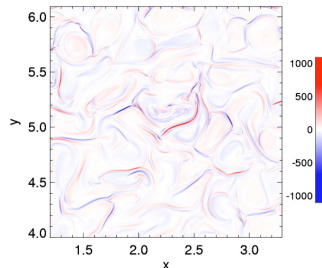


Figure 5: Current density of decaying MHD turbulence [Servidio et al., 2010]

# Spacecraft missions

- Recent in-situ measurements in turbulent space plasmas revealed the key role of **electrons** (before, mainly ions).
- Magnetospheric Multiscale Mission (MMS) measuring the plasmas of the Earth's magnetosphere
- Parker Solar Probe (PSP) measures the solar wind near the Sun.

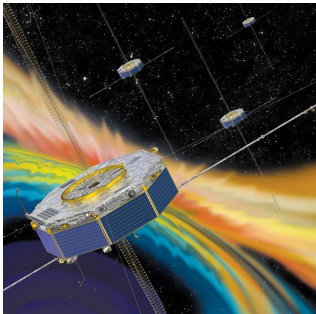


Figure 6: MMS

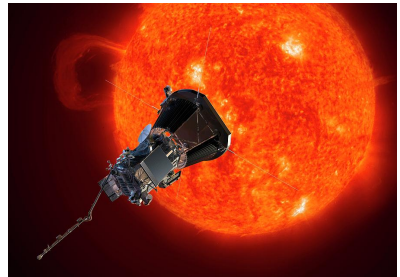


Figure 7: PSP

# Reconnection in turbulence

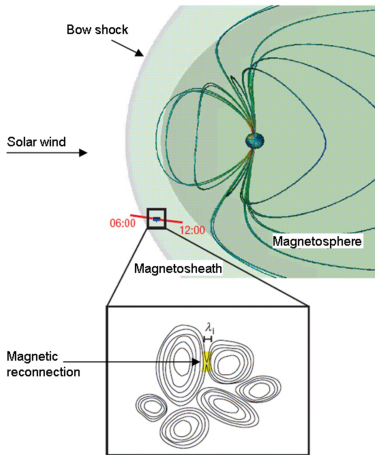


Figure 8: Small-scale magnetic reconnection in the turbulent magnetosheath

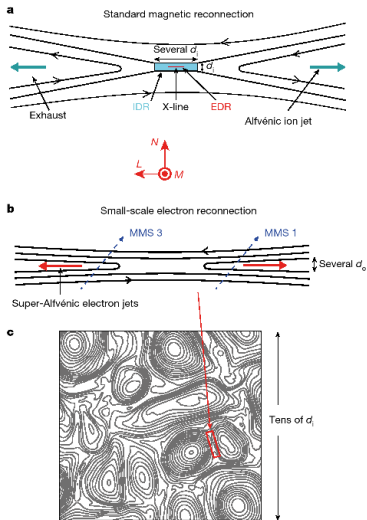


Figure 9: Schematics of electron-scale magnetic reconnection [Phan et al 2018]

# Open questions and purpose of this work

## Questions

- 1 Relevance of electron kinetic effects for the current sheet formation/magnetic reconnection in turbulence (dissipation/heating via instabilities)
- 2 Role of plasma-beta (thermal/magnetic pressure) on those effects (PSP can observe different plasma regimes near the Sun).

# Contents

- 1 Introduction
- 2 Method
  - Method
- 3 Results
- 4 Conclusions

# Numerical methods: Fully kinetic PIC code

## Fully kinetic PIC code

- Fully kinetic Vlasov-Maxwell system of equations.
- Particle-in-Cell Code ACRONYM (Advanced Code for Relativistic Objects, Now with Yee-Lattice and Macroparticles) [Kilian et al., 2012].
- 2nd order Maxwell solver, Boris pusher to advance particles, higher-order interpolation schemes.
- MPI parallelization, parallel HDF5 output.

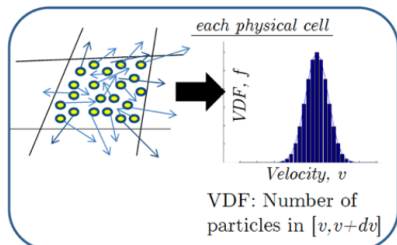
### Fully-kinetic equations

$$\nabla \times \vec{E} = -\frac{\partial \vec{B}}{\partial t}$$

$$\nabla \times \vec{B} = \mu_0 \vec{J} + \mu_0 \epsilon_0 \frac{\partial \vec{E}}{\partial t}$$

$$\left[ \frac{\partial}{\partial t} + \vec{v} \cdot \frac{\partial}{\partial \vec{x}} + \frac{q_\alpha}{m_\alpha} \left( \vec{E} + \vec{v} \times \vec{B} \right) \cdot \frac{\partial}{\partial \vec{v}} \right] f_\alpha = 0$$

+ Maxwell equations  $\nabla \cdot \vec{E}$  and  $\nabla \cdot \vec{B}$  and definitions of the sources  $\rho$  and  $\vec{J}$  as function of  $f$





# PiC loop

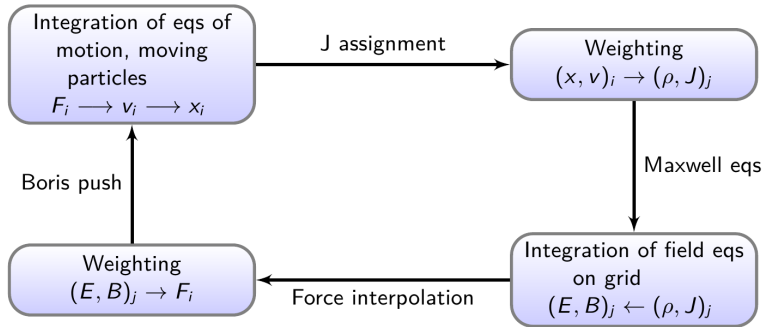


Figure 10: PiC loop

# Simulation setup of decaying collisionless turbulence

- 2D decaying turbulence simulations with out-of-plane background magnetic field  $\vec{B} = B_0 \hat{z}$
- Uncorrelated Alfvénic fluctuations  $\delta \vec{V}_\perp$  and  $-V_A \delta \vec{B}_\perp / B_0$ , wave modes initially excited:  $kd_i < 0.2$ , initial fluctuation amplitude  $B_{\text{RMS}} = 0.24 B_0$ .
- $m_i / m_e = 25$ ,  $\beta_e = \beta_i = 0.1$  and  $\beta_e = \beta_i = 2.0$
- Up to  $9600^2$  grid points,  $5.5 \times 10^{10}$  particles. Resources: 9.4k cores, 0.9M core-hours. Storage: 4.5 TB particle data per time snapshot.

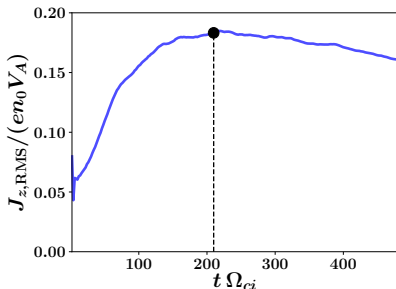


Figure 11: Time history of the RMS values of  $J_z$

# Contents

- 1 Introduction
- 2 Method
- 3 Results
  - Results
- 4 Conclusions

# Electron kinetic effects: low-beta

- A way to assess regions where electron kinetic effects are larger is the non-gyrotropy of the electron pressure tensor  $\bar{P}_e$ ,

$$D_{ng} = \sqrt{\sum_{i,j} (P_{ij,e} - G_{ij,e})^2 / \text{Tr}(\bar{P}_e)}$$
 (method by [Aunai et al., 2013].

$G_{ij,e}$  is the equivalent gyrotropic tensor.

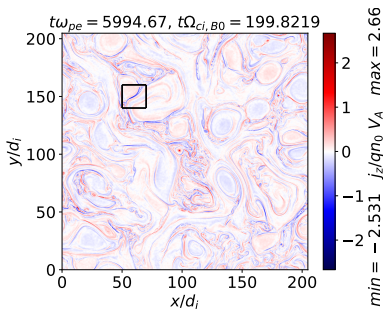


Figure 12:  $J_z$

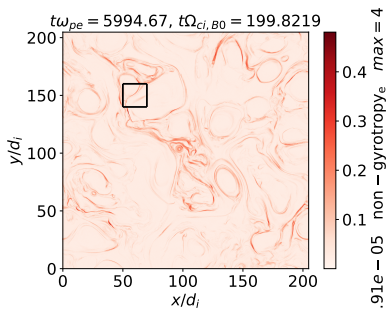


Figure 13:  $D_{ng}$

# Electron kinetic effects: low-beta

- A way to assess regions where electron kinetic effects are larger is the non-gyrotropy of the electron pressure tensor  $\bar{P}_e$ ,

$$D_{ng} = \sqrt{\sum_{i,j} (P_{ij,e} - G_{ij,e})^2 / \text{Tr}(\bar{P}_e)} \quad (\text{method by [Aunai et al., 2013]}).$$

$G_{ij,e}$  is the equivalent gyrotropic tensor.

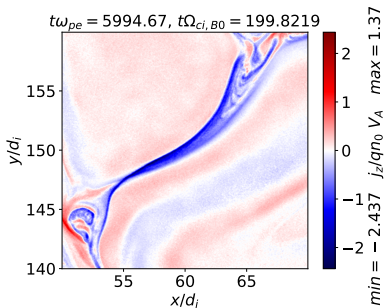


Figure 14: Zoomed-in  $J_z$

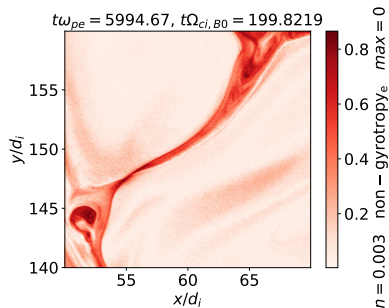


Figure 15: Zoomed-in  $D_{ng}$

# Distribution functions in the zoomed-in region

- Field-aligned double-peaked distribution functions with long plateaus near X-point. No streaming instabilities are possible though.
- The field-aligned double-peaked distribution functions with long plateaus can also be found in strong guide-field (3D) reconnection, but they are unstable!
- Non-field-aligned double peaked distribution functions near the downstream region

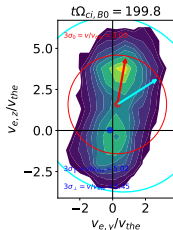


Figure 16: Near X-point @  $(56.6, 148.6)d_i$

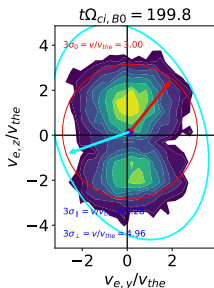


Figure 17: Downstream region @  $(65.6, 157.2)d_i$

# Plasma-beta effects

- Histograms of distribution of current-density and non-gyrotropy
- Higher plasma-beta tends to decrease the non-Maxwellian features and the current sheet strength (associated with smaller reconnection rates), temperature anisotropies, etc.

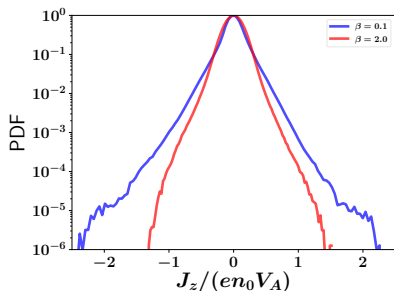


Figure 18:  $J_z$

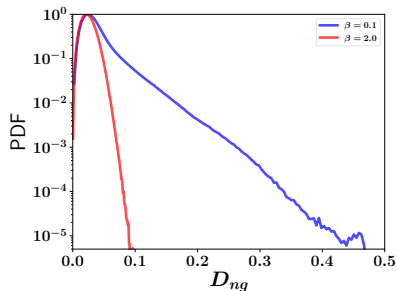


Figure 19:  $D_{ng}$

# Plasma-beta effects

- Higher plasma-beta tends to decrease the non-Maxwellian features and the current sheet strength (associated with smaller reconnection rates), temperature anisotropies, etc.

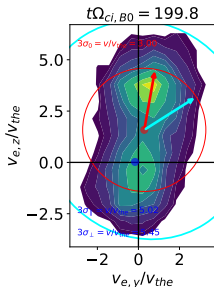


Figure 20: Near X-point, low- $\beta$

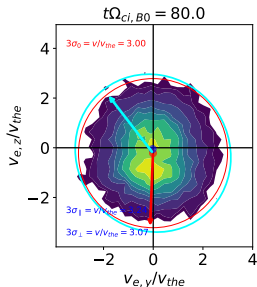


Figure 21: Near X-point, high- $\beta$



# Turbulent spectra

- What is the relation with turbulence?
- At kinetic scales the spectral index is 2.6 below ion-scales for the low beta plasma case, the same that is measured in space plasmas.
- Spectral power is enhanced at typical current sheet scales for the low-beta case.

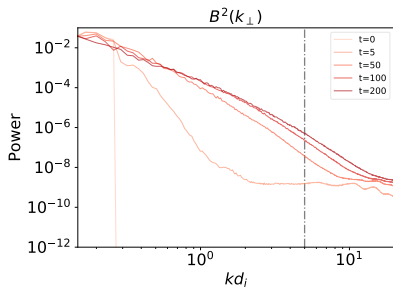


Figure 22: Low  $\beta$  evolution

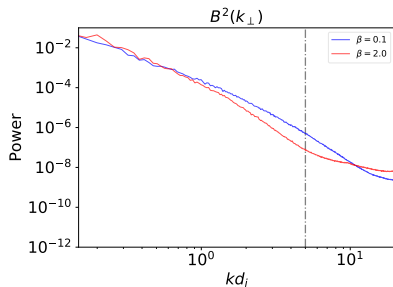


Figure 23: Comparison low vs high  $\beta$

# Contents

- 1 Introduction
- 2 Method
- 3 Results
- 4 Conclusions
  - Conclusions

# Conclusions

## Conclusions

- Fully kinetic (collisionless) decaying turbulence led to electron-scale current sheet formation
- Field-aligned double-peaked distribution functions in the neighborhood of current sheets, typical from strong-guide field reconnection, but no signatures of micro-instabilities.
- Higher plasma-beta tends to decrease the current sheet strength/peak values, the efficiency of magnetic reconnection in turbulence, and the non-Maxwellian features.

THE END

Thank you very much  
for your attention

Questions/Comments?

# Contents

## 5 Backup slides

# Bibliography I



Aunai, N., Hesse, M., and Kuznetsova, M. (2013).

Electron nongyrotropy in the context of collisionless magnetic reconnection.

*Phys. Plasmas*, 20(9):092903.



Kilian, P., Burkart, T., and Spanier, F. (2012).

The Influence of the Mass Ratio on Particle Acceleration by the Filamentation Instability.

In Nagel, W. E., Kröner, D. B., and Resch, M. M., editors, *High Perform. Comput. Sci. Eng. '11*, pages 5–13. Springer Berlin Heidelberg, Berlin, Heidelberg.



Matthaeus, W. H. and Lamkin, S. L. (1986).

Turbulent magnetic reconnection.

*Phys. Fluids*, 29(8):2513.



Servidio, S., Matthaeus, W. H., Shay, M. A., Dmitruk, P., Cassak, P. A., and Wan, M. (2010).

Statistics of magnetic reconnection in two-dimensional magnetohydrodynamic turbulence.

*Phys. Plasmas*, 17(3):032315.



Treumann, R. A. and Baumjohann, W. (2013).

Collisionless magnetic reconnection in space plasmas.

*Front. Phys.*, 1(M):1–34.